Surface & Coatings Technology xxx (xxxx) xxx–xxx

Contents lists available at ScienceDirect

Surface & Coatings Technology

journal homepage: www.elsevier.com/locate/surfcoat

Influence of microstructural features and deformation-induced martensite on hardening of stainless steel by cryogenic ultrasonic impact treatment

M.A. Vasylyev[a], B.N. Mordyuk[a,*], S.I. Sidorenko[b], S.M. Voloshko[b], A.P. Burmak[b]

[a] Department of Physical Fundamentals of Surface Engineering, Kurdyumov Institute for Metal Physics, NAS of Ukraine, 36 Academician Vernadsky Blvd., UA-03142 Kyiv, Ukraine

[b] Metal Physics Department, Igor Sikorsky National Technical University of Ukraine, 37 Peremohy ave., UA-03056 Kyiv, Ukraine

ARTICLE INFO

Keywords:
Stainless steel
Ultrasonic impact treatment
Cryogenic deformation
Martensitic transformation
Grain refinement
Hardness

ABSTRACT

Ultrasonic impact treatment of stainless steel AISI 321 was carried out at room temperature (in the argon environment – argon-UIT) and at cryogenic temperature (in liquid nitrogen – cryo-UIT) in the constrained conditions with application of the same mechanical energy to the treated specimens. The time dependencies of the surface hardness *HV* after the cryo-UIT and argon-UIT processes were of sigmoidal and parabolic shapes, respectively. The microstructural evolution of the surface layers of the deformed specimens was studied by X-ray diffraction (XRD), optical microscopy (OM), transmission electron microscopy (TEM) and selective area electron diffraction (SAED) analyses. The volume fractions of the deformation-induced α′ ($V_{\alpha'}$) and ε (V_{ε}) martensites were estimated using XRD approach and by magnetic and density measurements. Compared to the room temperature UIT in the argon environment (argon-UIT), the liquid nitrogen UIT generates a higher density of the deformation twins and stacking faults. In addition, a higher $V_{\alpha'}$ (~53%) and V_{ε} (~3.5%) were observed after cryo-UIT in deeper surface layers (~200 μm). The argon-UIT process leads to the formation of either rectangular twin blocks or dislocation cells, which size ranged 200–500 nm. Conversely, after cryo-UIT ($\bar{\varepsilon} \approx 0.95$), a nanoscale grain structure of heterogeneous nature (α′ and γ phases) was formed in the outmost surface layer simultaneously with the areas filled with networks of deformation twins and stacking faults. The minimum grain size of α′-martensite $D_{\alpha'}$ and austenite D_{γ} was respectively 25 and 45 nm, and twin thickness/spacing was of 60–120 nm. Both types of the microstructure contribute to the material strength and result in higher hardness of the cryo-UIT processed specimens (~5–5.66 GPa) compared to that of the argon-UIT processed ones (~4.3 GPa). With the increase in Zener-Hollomon parameter ln*Z*, the grain/twin/spacing size is decreased while the $V_{\alpha'}$ and surface microhardness *HV* are increased.

1. Introduction

Austenitic steels are widely used in industry due to its high resistance to corrosion, oxidation and high strength over a wide temperature range. These properties allow using these steels in biomedicine, chemical industry, and in the transportation facilities for liquefied natural gas, operating at cryogenic temperatures.

Accounting for the determinative role of the surface in the operational properties of materials and lifetime of constructions, one of the most important and widely studied areas is the mechanical modification of metallic surfaces using the methods of the surface severe plastic deformation (S^2PD). A lot of studies during the last decades demonstrate the beneficial effects of the surface nanostructurization on the anticorrosion property, wear resistance and fatigue durability of metallic materials. Several S^2PD methods, such as shot peening [1], surface mechanical attrition treatment (SMAT) [2–4], surface grinding [5], and ultrasonic impact treatment (UIT) [6–8] applied to stainless steels allow generating nanoscale grain structures in their surface layers, and significantly increase their physical and mechanical properties.

It is shown that among the factors leading to the mechanical nanostructuring, such as a high strain extent and high strain rate, the processing temperature is also an important parameter, which exerts a significant influence on the deformation mechanisms [9–12]. Thus, the temperature rise facilitating dynamic recrystallization (DRX) may limit the minimum grain size of the formed microstructure [13,14]. Additionally, the deformation heating can initiate phase transformations and facilitate further structural refinement through the strain induced heterogeneity of the phase composition in the surface layer. Conversely, the negative or cryogenic [12,15–18] temperatures applied at the SPD

* Corresponding author.
E-mail address: mordyuk@imp.kiev.ua (B.N. Mordyuk).

https://doi.org/10.1016/j.surfcoat.2017.11.019
Received 19 June 2017; Received in revised form 13 October 2017; Accepted 5 November 2017

(S^2PD) processes can essentially slow down the DRX or even almost completely hindered it. The outcome is the formation of ultrafine and/or nanoscale grain structures even in the materials of relatively low melting temperature (high DRX ability), such as copper [11,12], aluminium [19] and magnesium [20] alloys.

Cryogenic deformation of the stainless steels, particularly cryogenic tension [17,21–23], compression [24] or rolling [25], was shown to induce higher quantities of deformation twins, shear bands and stacking faults than those observed at room temperature. Strain induced epsilon- and alpha′-martensites were also formed more easily. The peculiarities of the strain induced structure and phase transformations in stainless steels at multiple impact loads were mainly analyzed in the ambient air (SMAT [2,3] or in the vacuum (UIT [6,7]). Only a few works were addressed to the outcomes of cryogenic SMAT [26] or cryogenic laser shock processing [27,28]. At the same time, the variation of the processing intensity and environmental/temperature conditions can be useful in the obtaining of new materials comprised both the microstructural and phase heterogeneities, which may provide the gradient mechanical and magnetic properties [29].

This work aims to study the microstructural features and phase transformations in stainless steel AISI 321 induced by the argon-UIT and cryogenic-UIT processes. The operative hardening mechanisms and the influence of Zener-Hollomon parameter were also addressed.

2. Experimental details

An austenitic stainless steel AISI-321, which chemical composition is given in Table 1, was used in this study. Disk specimens (thickness $h = 2$ mm and diameter $d = 6$ mm) of this steel were initially annealed for 1 h at 750 °C; the resulting initial average grain size was 50–100 μm. These specimens were exposed to UIT at different processing temperatures.

Details of the UIT process can be found elsewhere [6–8,30–33]. In this study, ultrasonic equipment schematically shown in Fig. 1 contained an ultrasonic generator with a frequency of 21.6 kHz and a power output of 0.6 kW. The cylindrical pin positioned between the tip of an ultrasonic horn and the specimen produced repetitive impacts by the treated surface. Impacts frequency induced by vibration of the ultrasonic horn was of ~1–2 kHz. The specimen was placed into a socket made in the hardened steel holder and underwent the quasi-hydrostatic shock compression during each impact. The estimated strain rate ranges 0.1–1.5 s^{-1} and decrease far from the treated surface. The UIT process lasted from 50 to 250 s and induced severe plastic deformation of the specimen surface and near the surface area. Two series of similar specimens were processed: the first one in the argon environment (argon-UIT) and the second one in liquid nitrogen (cryo-UIT). A special sealed chamber [31,33,34] filled with gaseous argon or liquid nitrogen was used (Fig. 1).

During each impact, the treated specimen was restricted in every direction except for a minor outflow of the surface layer which occurs around the outer edge of the treated disk specimen, i.e. the deformation occurs in so-called quasi-isostatic conditions (Fig. 1b). To estimate the effective strain $\bar{e}$, the following expression was used [30,35]:

$$\bar{e} = (\sqrt{2}/3)[(\varepsilon_1-\varepsilon_2)^2 + (\varepsilon_2-\varepsilon_3)^2 + (\varepsilon_3-\varepsilon_1)^2]^{1/2} \quad (1)$$

where $\varepsilon_1 = (h_0 - h_P)/h_0$, $\varepsilon_2 = \varepsilon_3 = (d_0 - 2p)/d_0$ are the principal strains, h_0 and h_P are thicknesses of the initial and as-treated disk-samples measured on their axis, d_0 is an initial diameter of the disk-sample, and p is a height of the pileup formed around the outer edge of the treated disk-sample after the UIT processing for a certain time.

Table 1
Chemical composition of the stainless steel AISI-321 (wt%, balance is Fe).

C	Si	Mn	Cr	Ni	Ti	P	S
≤ 0.07	≤ 0.8	1–2	17–19	9–11	0.7	< 0.03	< 0.02

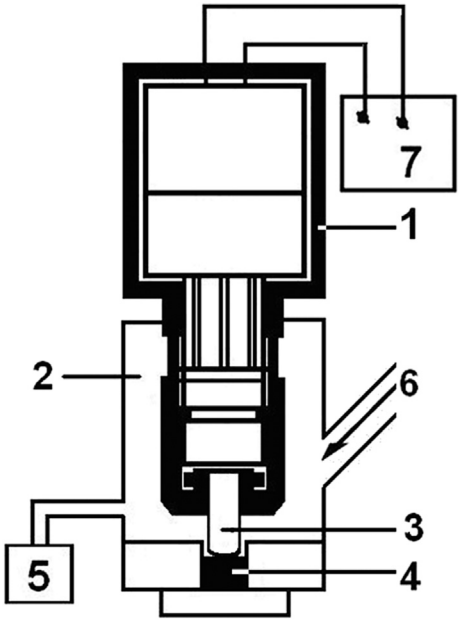

Fig. 1. Scheme of the specimen loading unit at the UIT process: 1 is the ultrasonic transducer with a step-like horn; 2 is a hermetic chamber; 3 is a pin; 4 is a disc-specimen; 5 is manometer; 6 is a channel used for filling of the chamber with gas or liquid nitrogen; 7 is an ultrasonic generator.

Microhardness HV of the surfaces and cross-sections were respectively measured at loads of 100 and 20 g and a dwell time of 10 s using a PMT-3M microdurometer.

Since the UIT process was performed at different temperatures in this study, the Zener-Hollomon parameter representing the combined effect of strain rates ($\dot{\varepsilon}$) and deformation temperatures (T) was calculated using the well-known expression [11,12]:

$$\ln Z = \ln \dot{\varepsilon} + \ln(Q/RT). \quad (2)$$

Using the activation energy for deformation of this stainless steel $Q \approx 33.4$ kJ/mol adopted after [36] the ln$Z$ estimations were performed for experimental conditions used both in this study and in the literature (see Table 2).The actual sample temperature (T) is normally larger than the nominal deformation temperature due to the transient temperature rise ΔT induced by plastic deformation, which can be accounted for as follows [11,30]:

$$\Delta T = (\beta/C_V m\rho) \int_{\bar{e}_1}^{\bar{e}_2} \sigma_Y \bar{e} \mathrm{d}\bar{e}, \quad (3)$$

where β ≈ 0.9–0.95 is a factor for conversion of the deformation work done into heat, ρ is the density, C_V is the specific heat capacity, σ_Y is the yield stress that correlates to the Vickers hardness through the Tabor's relation $\sigma_Y \approx 0.3HV$, $\bar{e}$ is the effective strain. This expression is valid in our case owing to the adiabatic character of the UIT process (high strain rate and very short deformation duration during each impact).

Microstructural analysis of the surface layers was performed using optical microscopy (OM), X-ray diffraction (XRD) analysis, transmission electron microscopy (TEM) and selective area electron diffraction (SAED) studies.

Optical metallography of the cross-sections of the original and treated specimens was carried out using a Neophot-32 microscope. The grain boundaries were etched using a NITAL reagent.

TEM observations and SAED studies were carried out using a JEM 100 CX-II microscope. The plane-view TEM foils were prepared from different sections of treated specimens (the top surface layer and ~30 μm from the outer surface). They were mechanically polished on the untreated side of the sample followed by electro-polishing by means of a twin-jet technique. One-side polishing was used to obtain the foil